Research Square

Preprints are preliminary reports that have not undergone peer review.
They should not be considered conclusive, used to inform clinical practice,
or referenced by the media as validated information.

Development of a Method for Dividing Mountainous Regions into Windward and Leeward Areas According to Wind Direction

Keisuke Watanabe

keisukewatanabe528@keio.jp

Keio University

Yoshiaki Miyamoto

Keio University

Short Report

Keywords: Windward and leeward classification, Orographic precipitation, Digital elevation model (DEM), Wind direction, Mountainous regions

Posted Date: November 19th, 2026

DOI: https://doi.org/10.21203/rs.3.rs-11676151/v1

License: This work is licensed under a Creative Commons Attribution 4.0 International License.
Read Full License

Additional Declarations: No competing interests reported.

Development of a Method for Dividing Mountainous Regions into Windward and Leeward Areas According to Wind Direction

Keisuke Watanabe[1*]

ORCID id: 0009-0005-5424-9244

Correspondence: keisukewatanabe528@keio.jp

Yoshiaki Miyamoto[2]

Author details

1 Graduate School of Media and Governance, Keio University, 5322 Endo, Fujisawa, Kanagawa, 252-0882, Japan

2 Faculty of Environment and Information Studies, Keio University, 5322 Endo, Fujisawa, Kanagawa, 252-0882, Japan

Abstract

Precipitation in mountainous regions is strongly influenced by wind direction and is generally enhanced on windward slopes and reduced on leeward slopes. However, definitions of windward and leeward areas vary among previous studies, and objective

methods for spatially classifying complex mountainous regions according to arbitrary wind directions remain limited. This study proposes a windward–leeward classification method using high-resolution elevation and official summit-location data. Summit-based mountain areas were constructed, and high-elevation lines within individual mountain areas were combined with boundaries between adjacent mountain areas to classify windward and leeward areas. The method was applied to Kyushu, Japan, for 16 wind directions. The resulting classifications were evaluated using precipitation and 850-hPa wind data from the Meso-Scale Model Grid Point Value dataset (MSM-GPV). Mean precipitation was greater on the windward side in all 25 mountain areas analyzed, with statistically significant differences in 23 areas. These results indicate that the proposed method produces classifications consistent with the expected windward–leeward precipitation contrast and provides a basis for spatial analyses of precipitation in complex mountainous regions according to wind direction.

Keywords

Windward and leeward classification, Orographic precipitation, Digital elevation model (DEM), Wind direction, Mountainous regions

Statements and Declarations

Competing interests

The authors declare that they have no competing interests.

1 Introduction

Precipitation in mountainous regions can cause disasters such as landslides and floods, making it important for disaster risk reduction to accurately characterize and predict its spatial distribution. However, the spatial distribution of precipitation in mountainous regions remains difficult to characterize and predict because of limited observations and the influence of complex terrain (Stuart et al. 2025). Precipitation distributions in mountainous regions are affected by geographical and topographic factors, such as elevation, slope, and distance from the coast (Basist et al. 1994; Johansson and Chen 2003), as well as meteorological factors, such as wind direction, wind speed, atmospheric stability, and water vapor (Eidhammer et al. 2018; McMurdie et al. 2018). In particular, when moist air encounters mountainous terrain, it is forced to ascend, promoting condensation and cloud development and thereby producing orographic precipitation. Although precipitation maxima can occur near mountain summits or on the leeward side depending on factors such as hydrometeor advection, mountain width, wind speed, and atmospheric stability, precipitation is generally enhanced on the windward side by orographic lifting and suppressed on the leeward side by descending airflow and reduced moisture (Roe 2005). Therefore, analyzing precipitation

distributions in mountainous regions requires appropriate identification of whether each location lies on the windward or leeward side according to wind direction.

Various approaches have been used to distinguish or evaluate windward and leeward areas in mountainous regions. These include dividing windward and leeward areas using major ridgelines or opposing mountain slopes (Singh et al. 1995; Suprit and Shankar 2008), evaluating orographic lifting using slope aspect or wind-direction-dependent terrain gradients (Johansson and Chen 2003; Shetty et al. 2022), quantifying terrain shelter and exposure due to upwind barriers (Yin et al. 2008; Brenner et al. 2026), and analyzing windward and leeward effects using airflow fields and vertical motion simulated by numerical models (Jiang 2003; Mott and Lehning 2010). However, definitions and approaches for identifying windward and leeward areas vary among studies (Zaujec et al. 2025). Methods for objectively classifying individual locations as windward or leeward according to arbitrary wind directions remain limited, particularly for broad mountainous regions containing multiple mountains and complex ridgelines.

Various methods have also been proposed to extract mountainous regions and terrain features from digital elevation models (DEMs). Examples include detecting summits based on elevation differences from surrounding locations or topographic prominence

(Torres et al. 2018); classifying terrain into landform types such as summits, ridges, slopes, and valleys using terrain metrics or the relative position and configuration of elevation within the surrounding terrain (Szypuła 2019; Gupta and Dixit 2024); delineating and characterizing terrain units based on watershed and drainage-divide structures (Lin et al. 2021; Jancewicz et al. 2022); and delineating terrain features using object-based approaches (Drăguţ et al. 2011). These studies provide a range of approaches for delineating mountainous regions and terrain features from DEMs. Building on these advances, a further step for analyzing mountainous precipitation in relation to wind direction is to spatially classify locations within the delineated mountainous regions as windward or leeward while accounting for terrain structure.

In this study, rather than proposing a new method for extracting mountainous regions themselves, we propose a method for spatially classifying locations as windward or leeward according to wind direction based on explicit criteria, using mountainous regions defined from high-resolution elevation data and official summit-location data. After defining a mountain area corresponding to each summit, the method combines boundaries representing ridgelines within individual mountain areas with boundaries between adjacent mountain areas to classify windward and leeward areas for each wind direction. We further examine the meteorological consistency of the classification by

comparing precipitation between windward and leeward areas of multiple mountains using precipitation data from a numerical weather prediction model. The objective is to provide a basis for spatially analyzing the relationship between precipitation distributions and wind direction in mountainous regions containing multiple mountains and complex ridgelines.

2 Data and Method

2.1 Study Area

Mainland Kyushu, Japan, was selected as the case-study region for the proposed method. Kyushu contains multiple mountainous regions, including areas where summits and mountains are located close to one another. Consequently, its complex terrain structure is difficult to represent using a single major ridgeline. In addition, mainland Kyushu contains multiple mountainous regions at a spatial scale that allows detailed examination of the classification results, making it suitable for evaluating the applicability of the proposed windward–leeward classification method. Figure 1 shows the study area and the summit locations used in the analysis.

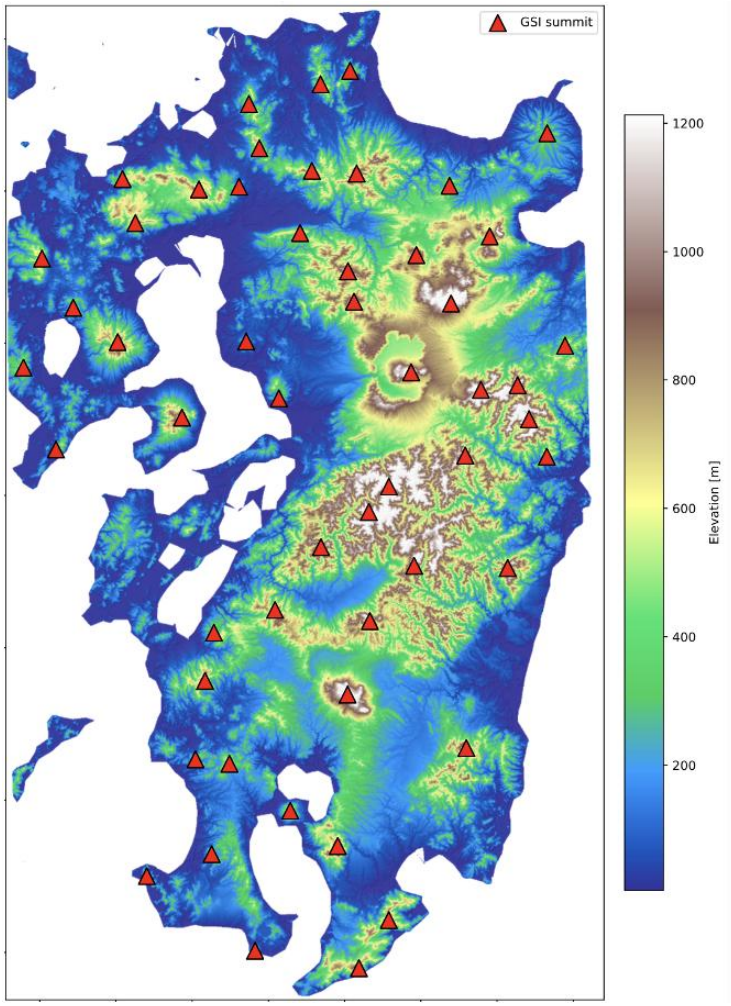


Fig. 1 Study area and selected summit locations used in this study. The shaded colors indicate elevation based on the 25 m DEM created from GSI elevation point data. Red triangles indicate summit locations selected from the GSI list of major mountains in Japan.

2.2 Data

For distance-based terrain processing, including construction of the 25 m grid, calculation of distances between summits, and definition of strip-shaped regions, the elevation and summit-location data were transformed to UTM Zone 52N (EPSG:32652).

2.2.1 Elevation data

Elevation data were obtained from the elevation points included in the Fundamental Geospatial Data (Basic Items) provided by the Geospatial Information Authority of Japan (GSI 2026a). Because the elevation points are irregularly distributed, a Delaunay triangulation was constructed, and a gridded DEM with a 25 m spacing was generated by TIN-based linear interpolation. Locations where reliable interpolation was difficult, such as areas with sparse elevation points, were treated as missing values and excluded from subsequent analyses.

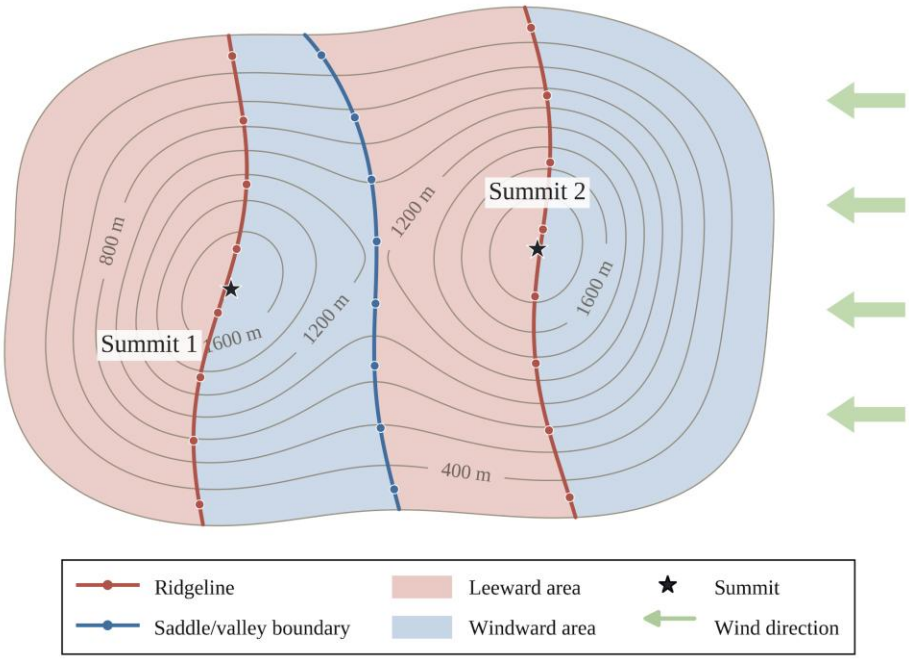
2.2.2 Summit location data

Summit-location data were obtained from the GSI dataset Elevation of the Principal Mountains in Japan—1003 Mountains (GSI 2026b). This dataset provides mountain

130 names, locations of the highest points, elevations, and other information for 1003 major
131 mountains in Japan based on fundamental surveying products, including 1:25,000-scale
132 topographic maps. Summits located on mainland Kyushu were extracted and used as
133 seed points for constructing summit-based mountain areas. To avoid excessive
134 subdivision of mountain areas due to closely spaced summits, when multiple summits
135 were located within 10 km of one another, only the summit with the highest elevation
136 was retained.

137 **2.3 Overview of the windward–leeward classification**

138 The proposed method uses two types of boundaries to separate windward and leeward
139 areas: boundaries representing ridgelines within individual mountain areas and
140 boundaries corresponding to saddles or valleys between adjacent mountain areas (Fig.
141 2). For each wind direction, these boundaries were combined, and the upwind side was
142 classified as windward and the opposite side as leeward.



143

144 **Fig. 2** Conceptual diagram of the windward–leeward classification method under

145 easterly wind conditions. Red lines and markers indicate ridgelines within individual

146 mountain areas, and the blue line and markers indicates a saddle/valley boundary

147 between adjacent mountain areas. Blue and red shaded areas indicate windward and

148 leeward areas, respectively. Green arrows indicate wind direction.

149 **2.4 Construction of summit-based mountain areas and inter-mountain boundaries**

150 To define a mountain area corresponding to each summit, grid cells were progressively

151 assigned to individual summits from higher to lower elevations, using the summit

152 locations as seed points. First, grid cells at elevations of 1000 m or higher were

153 extracted, and cells connected using an eight-neighbor criterion were treated as a

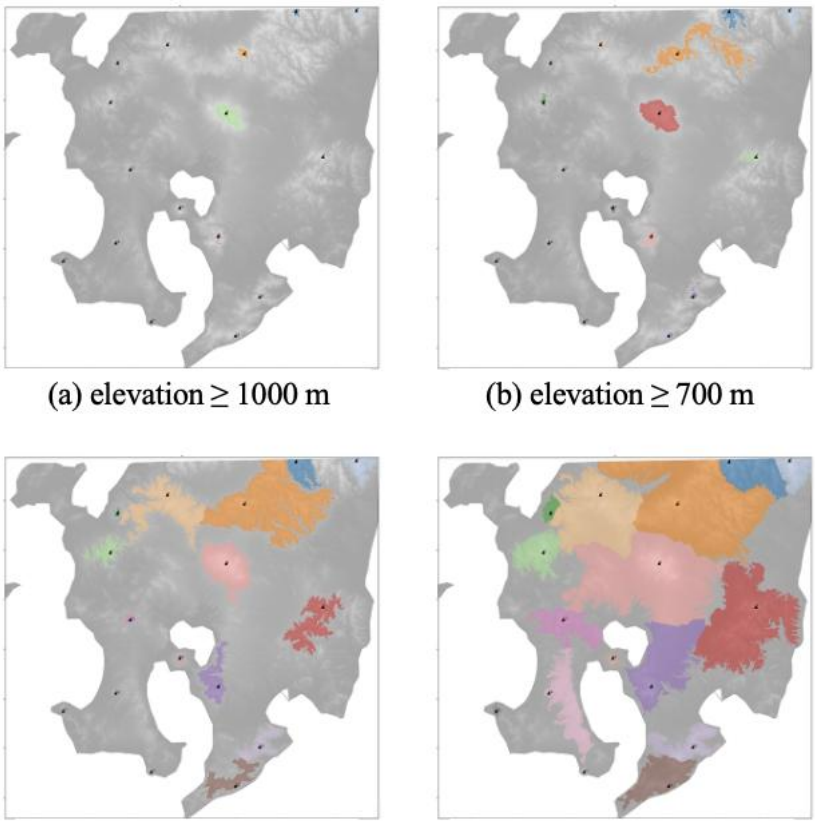
154 contiguous region. If a contiguous region contained a summit, it was assigned to the
155 mountain area associated with that summit; otherwise, it was treated as a neutral region.

156 The same procedure was then repeated while lowering the elevation threshold in 50 m
157 increments. When a newly identified contiguous region or a neutral region contacted an
158 existing mountain area, it was merged into that mountain area. When a region contacted
159 multiple mountain areas, each grid cell was assigned to the mountain area of the nearest
160 summit. This procedure was repeated down to an elevation of 150 m, and locations
161 below 150 m were treated as outside the mountain areas and excluded from the
162 windward–leeward classification. Figure 3 shows an example of the stepwise
163 construction of mountain areas in southern Kyushu.

164 By progressively lowering the elevation threshold, mountain areas expanded from high-
165 elevation regions surrounding each summit toward lower elevations, forming
166 boundaries where adjacent mountain areas met. These boundaries were treated as
167 boundaries corresponding to saddles or valleys between adjacent mountains and were
168 used to define transitions between windward and leeward areas.

169 Previous studies have used hydrological analysis of digital elevation models (DEMs) to
170 delineate watershed boundaries (Jenson and Domingue, 1988), and this approach has

171 also been applied to inverted DEMs to divide mountainous terrain into individual
172 mountain units (Zhang et al., 2022). In contrast, the present study employed a summit-
173 based approach that progressively expanded mountain areas from higher to lower
174 elevations according to predefined rules, without requiring hydrological flow analysis or
175 manual boundary adjustment.



176

177 **Fig. 3** Example of the stepwise construction of summit-based mountain areas in
178 southern Kyushu. Colored areas indicate mountain areas assigned to each summit, and
179 black triangles indicate summit locations. As the elevation threshold decreases from (a)

1000 m to (d) 150 m, mountain areas expand from high-elevation regions around the summits toward lower-elevation areas.

2.5 Extraction of ridgelines and classification of windward and leeward areas

To define boundaries separating windward and leeward areas within each mountain area, a representative line of the internal ridgeline was extracted for each wind direction. First, strip-shaped regions oriented parallel to the wind direction were defined within each mountain area at 500 m intervals in the direction perpendicular to the wind. The highest-elevation point within each strip was then extracted as a representative high-elevation point. This procedure identified a sequence of representative points along the high-elevation portion of the mountain in the direction perpendicular to the wind.

Strips with representative high-elevation points below 200 m were excluded to prevent low-elevation areas from being identified as ridgelines. In addition, to remove isolated representative high-elevation points separated from the continuous high-elevation region, horizontal distances were calculated from each point to up to 10 points before and after it along the sequence of strips. If eight or more of these points were located at least 10 km from the target point, the target point was classified as isolated and excluded.

The locations of the remaining representative high-elevation points were smoothed using a moving average based on each point and its two adjacent points. The smoothed points were then connected sequentially to construct a representative line of the ridgeline within the mountain area. Strips from which isolated points had been removed were interpolated using representative points in the two adjacent strips. However, strips excluded because their representative high-elevation points were below 200 m were not interpolated. Figure 4 shows an example for a single mountain area, illustrating the extraction of representative high-elevation points and the construction of the representative and classification lines.

For the windward–leeward classification, the representative line was shifted 0.5 km leeward to define the classification line so that locations on and near the ridgeline were included on the windward side. The offset distance was set to 0.5 km, corresponding to the strip spacing used for representative-line extraction. The upwind side of the classification line was classified as windward, and the opposite side as leeward. The classification lines within mountain areas were then combined with the boundaries between adjacent mountain areas to classify the entire study area as windward or leeward. This procedure was applied to each of 16 wind directions to generate wind-direction-dependent classifications.

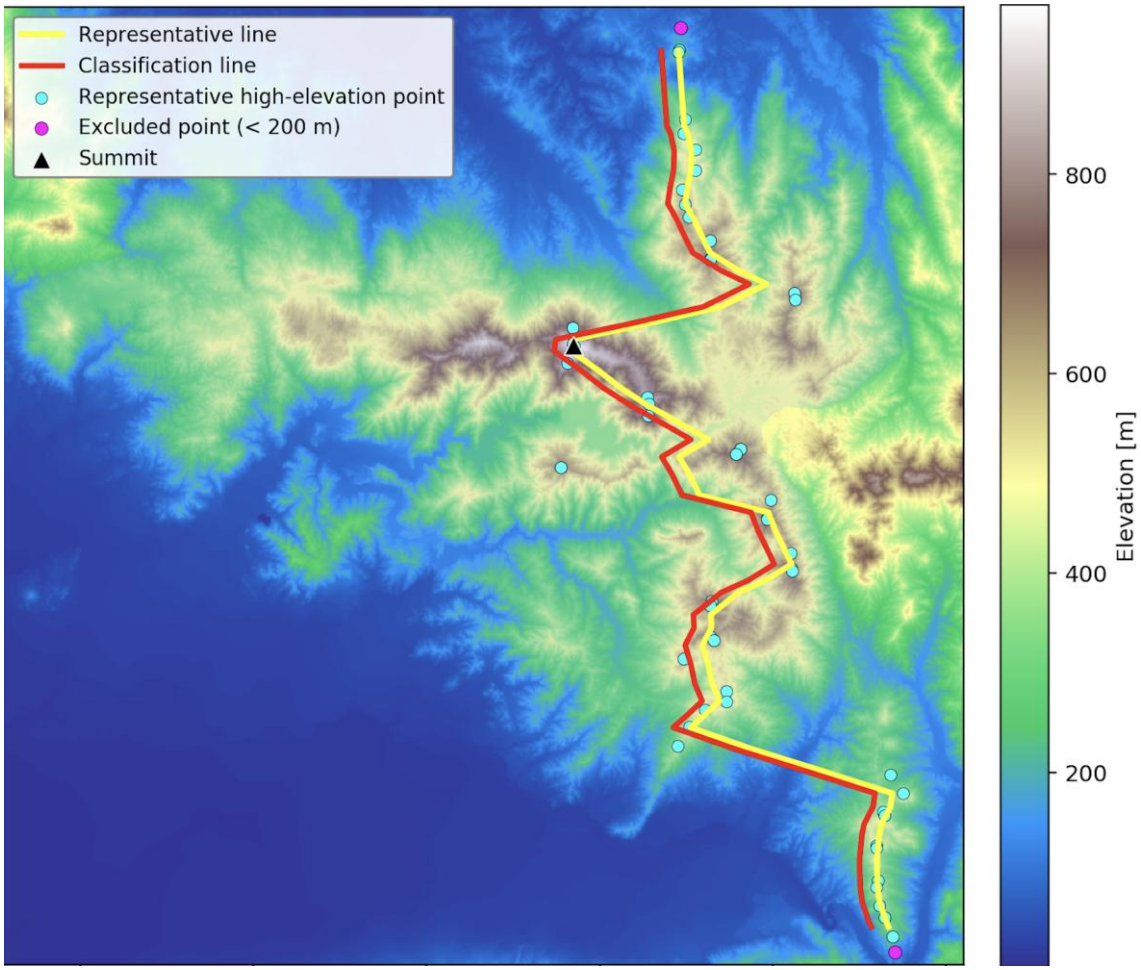


Fig. 4 Example of representative-line extraction within a mountain area under easterly wind conditions. Cyan points indicate representative high-elevation points extracted from each strip, and magenta points indicate excluded points with elevations lower than 200 m. The yellow line indicates the representative line constructed from the smoothed representative high-elevation points, and the red line indicates the classification line shifted 0.5 km leeward from the representative line. The black triangle indicates the summit location.

2.6 Comparison of precipitation between windward and leeward areas

To examine the correspondence between the proposed classification and precipitation distributions, precipitation and 850 hPa wind data from the Meso-Scale Model Grid Point Value dataset (MSM-GPV) provided by the Japan Meteorological Agency (JMA 2026) were analyzed for the period from April 2015 to March 2020. The MSM-GPV data had a spatial resolution of 5 km and a temporal interval of 3 h. To avoid mean precipitation on either side being determined by a single MSM-GPV grid point, 25 of the 53 mountain areas, each containing at least two MSM-GPV grid points on both the windward and leeward sides for all 16 wind directions, were selected for analysis.

For each mountain area, times when the area-mean 3-h accumulated precipitation was at least 1 mm were extracted. The zonal and meridional wind components at 850 hPa were spatially averaged over each mountain area at each selected time, and the resulting mean wind direction was classified into one of 16 directions. Using the classification corresponding to this wind direction, each MSM-GPV grid point was classified as windward or leeward, and mean precipitation for each side was calculated over all selected times.

The statistical significance of the precipitation difference between the windward and leeward sides was evaluated using a label-flipping permutation test, with the paired windward and leeward precipitation values at each selected time treated as the unit of permutation. The windward and leeward labels were randomly flipped at each selected time, and this procedure was repeated 10,000 times. The difference in mean precipitation between the two sides was recalculated for each permutation to construct the null distribution under the hypothesis of no systematic difference between windward and leeward precipitation. A one-sided p value was then calculated for the alternative that mean precipitation was greater on the windward side than on the leeward side.

3 Results

3.1 Windward–leeward classification

Figure 5 shows the windward–leeward classification for mainland Kyushu under easterly wind conditions. Blue and red indicate windward and leeward areas, respectively; gray indicates unclassified areas; black lines indicate boundaries between adjacent mountain areas; and black triangles indicate summit locations. Under easterly wind conditions, the eastern side of each mountain area was generally classified as

windward and the western side as leeward. However, where multiple mountains were located close to one another, the windward–leeward distribution did not simply divide the entire study area into eastern and western halves but varied spatially according to the boundaries defined within individual mountain areas and between adjacent mountain areas. Thus, a spatial windward–leeward classification corresponding to easterly winds was obtained for the mountainous regions of mainland Kyushu.

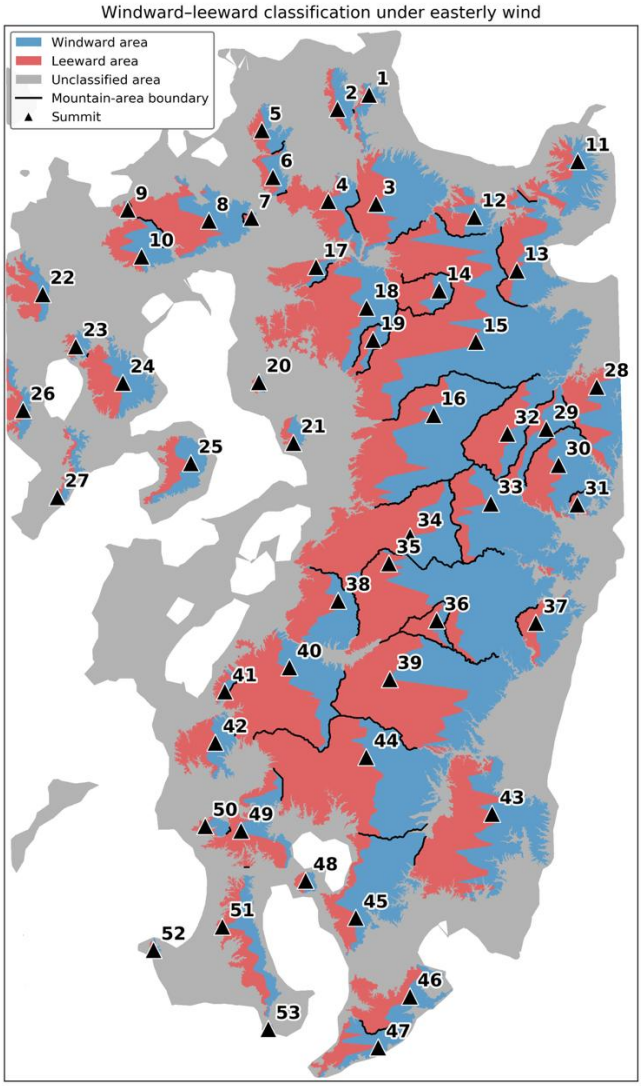
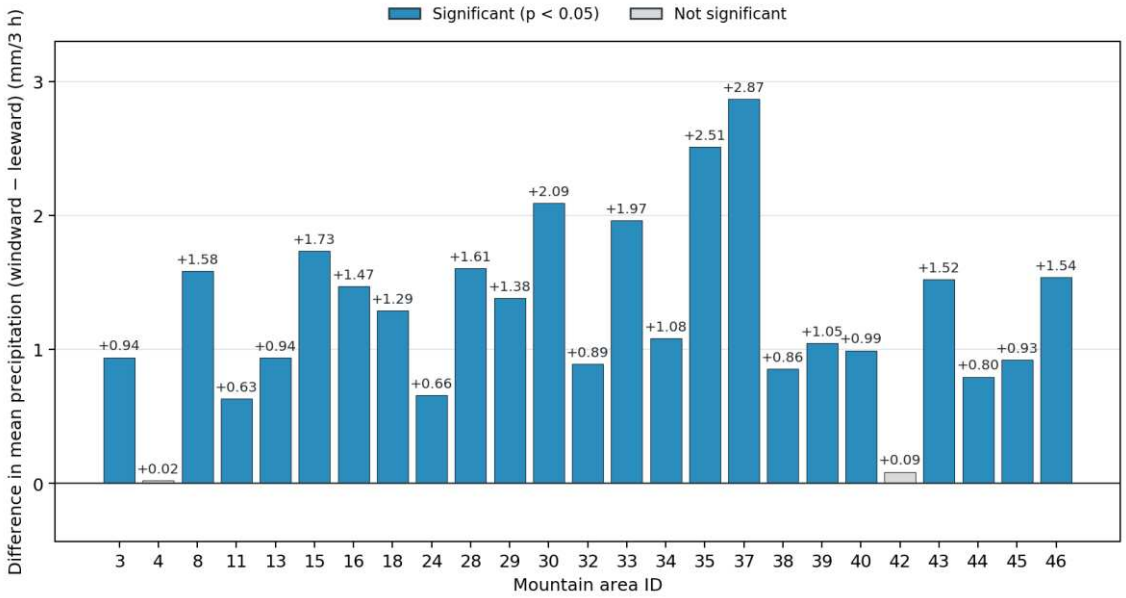


Fig. 5 Windward–leeward classification result under easterly wind conditions. Blue and red areas indicate windward and leeward areas, respectively, and gray areas indicate unclassified areas. Black lines indicate boundaries between adjacent mountain areas, and black triangles indicate summit locations. Numbers indicate mountain area IDs corresponding to the summit locations.

3.2 Precipitation differences between windward and leeward areas

Figure 6 shows the differences in mean precipitation between the windward and leeward sides for each mountain area analyzed. The differences were positive for all 25 mountain areas, indicating greater mean precipitation on the windward side than on the leeward side. The differences varied among mountain areas, ranging from 0.02 to 2.87 mm/3 h. The label-flipping permutation test based on paired precipitation values at each selected time showed that mean precipitation was significantly greater on the windward side in 23 of the 25 mountain areas ($p < 0.05$).



276

277 **Fig. 6** Differences in mean precipitation between windward and leeward areas for each

278 mountain area. Mountain area IDs correspond to those shown in Fig. 5. Positive values

279 indicate greater mean precipitation on the windward side than on the leeward side. The

280 numbers above the bars indicate the precipitation differences (windward − leeward).

281 Blue bars indicate statistically significant differences ($p < 0.05$), whereas gray bars

282 indicate non-significant differences, based on one-sided label-flipping permutation tests.

283

284

4 Discussion

Comparison of the classification results with precipitation distributions showed that mean precipitation was greater on the windward side than on the leeward side in all 25 mountain areas analyzed. However, the label-flipping permutation test did not indicate a statistically significant difference for some mountain areas. Nevertheless, the consistent direction of the precipitation differences across all mountain areas is consistent with the general characteristic of orographic precipitation, in which orographic lifting of moist airflow enhances precipitation on the windward side. Thus, at least in comparison with MSM-GPV precipitation distributions over Kyushu, the classifications produced by the proposed method were consistent with the expected windward–leeward contrast in orographic precipitation.

The proposed method includes several parameters that must be specified according to the terrain characteristics and spatial scale of the analysis, including summit selection, the minimum elevation defining mountain areas, criteria for excluding representative high-elevation points, and the spacing of strip-shaped regions. In particular, the number of selected summits affects the degree of subdivision of mountain areas: a larger number of summits results in classifications that represent more local terrain structures,

whereas a smaller number represents broader-scale mountain structures. These parameters should therefore be selected with consideration of the terrain characteristics of the study region and the spatial scale of the phenomenon being analyzed.

The method also assigns a representative wind direction to each mountain area and therefore assumes that wind direction is spatially uniform around the mountain. Local variations in airflow caused by terrain, such as flow deflection and flow around mountains, are not considered. In regions with complex terrain or closely spaced mountains, local airflow directions may differ from the representative wind direction. Future comparisons with airflow fields from high-resolution numerical models are needed to examine how such local airflow variations affect the classification results.

Furthermore, the MSM-GPV data used to evaluate the classification have a spatial resolution of 5 km and may therefore be insufficient to represent the detailed windward–leeward distributions derived from the 25 m DEM. Although the mountain areas analyzed in this study were restricted to reduce this effect, future work should examine the correspondence between the classification and precipitation distributions using higher-resolution meteorological or observational data and assess the applicability of the method to regions with different terrain characteristics.

5 Summary

This study proposed a method for classifying individual locations in mountainous regions as windward or leeward according to wind direction using a high-resolution DEM and summit-location data, with the aim of spatially analyzing the relationship between precipitation distributions and wind direction. Summit-based mountain areas were constructed, and representative lines of ridgelines within individual mountain areas were combined with boundaries between adjacent mountain areas to classify windward and leeward areas even in complex mountainous regions containing closely spaced mountains. By applying this procedure to 16 wind directions, wind-direction-dependent classifications were generated without prescribing a particular prevailing wind direction or a single major ridgeline.

To examine the correspondence between the proposed classification and precipitation distributions, windward and leeward precipitation were compared using MSM-GPV precipitation and 850 hPa wind data. Mean precipitation was greater on the windward side in all mountain areas analyzed. These results indicate that the classifications produced by the proposed method are consistent with the windward–leeward

precipitation contrast expected for orographic precipitation and can provide a basis for spatial analyses of the relationship between precipitation distributions and wind direction in mountainous regions.

Acknowledgements

This work was supported by JST SPRING, Japan Grant Number JPMJSP2123. The MSM data used in this study were collected and distributed by Research Institute for Sustainable Humanosphere, Kyoto University (http://database.rish.kyoto-u.ac.jp/index-e.html).

References

Basist A, Bell GD, Meentemeyer V (1994) Statistical relationships between topography and precipitation patterns. J Clim 7(9):1305–1315. https://doi.org/10.1175/1520-0442(1994)007<1305:SRBTAP>2.0.CO;2

Brenner J-B, Quiquet A, Roche DM, Paillard D, Vaittinada Ayar P (2026) GeoDS (v.1.0): a simple Geographical DownScaling model for long-term precipitation data over complex terrains. Geosci Model Dev 19(3):1075–1101. https://doi.org/10.5194/gmd-19-1075-2026

353 Drăguţ L, Eisank C, Strasser T (2011) Local variance for multi-scale analysis in
354 geomorphometry. Geomorphology 130(3–4):162–172.
355 https://doi.org/10.1016/j.geomorph.2011.03.011
356 Eidhammer T, Grubišić V, Rasmussen R, Ikdea K (2018) Winter precipitation efficiency
357 of mountain ranges in the Colorado Rockies under climate change. J Geophys Res
358 Atmos 123(5):2573–2590. https://doi.org/10.1002/2017JD027995
359 Geospatial Information Authority of Japan (GSI) (2026a) Fundamental Geospatial Data
360 Download Service. https://service.gsi.go.jp/kiban/app/. Accessed 3 October 2026
361 Geospatial Information Authority of Japan (GSI) (2026b) Elevation of the principal
362 mountains in Japan—1003 mountains.
363 https://www.gsi.go.jp/kihonjohochousa/kihonjohochousa41139.html. Accessed 3
364 October 2026
365 Gupta L, Dixit J (2024) Investigating the spatial distribution of flood inundation and
366 landforms using topographic position index (TPI) and geomorphon-based automated
367 landform classification methods. J Earth Syst Sci 133(3):126.
368 https://doi.org/10.1007/s12040-024-02343-x
369 Japan Meteorological Agency (JMA) (2026) Meso-Scale Model. JMA Information
370 Catalogue. https://www.data.jma.go.jp/add/suishin/cgi-

371 bin/catalogue/make_product_page.cgi?id=MesModel. Accessed 3 October 2026
372 Jenson SK, Domingue JO (1988) Extracting topographic structure from digital elevation
373 data for geographic information system analysis. Photogramm Eng Remote Sens
374 54(11):1593-1600.
375 Jiang Q (2003) Moist dynamics and orographic precipitation. Tellus A 55(4):301–316.
376 https://doi.org/10.1034/j.1600-0870.2003.00025.x
377 Johansson B, Chen D (2003) The influence of wind and topography on precipitation
378 distribution in Sweden: statistical analysis and modelling. Int J Climatol
379 23(12):1523–1535. https://doi.org/10.1002/joc.951
380 McMurdie LA, Rowe AK, Houze RA Jr, Brodzik SR, Zagrodnik JP, Schuldt TM (2018)
381 Terrain-enhanced precipitation processes above the melting layer: Results from
382 OLYMPEX. J Geophys Res Atmos 123(21):12194–12209.
383 https://doi.org/10.1029/2018JD029161
384 Mott R, Lehning M (2010) Meteorological modeling of very high-resolution wind fields
385 and snow deposition for mountains. J Hydrometeorol 11(4):934–949.
386 https://doi.org/10.1175/2010JHM1216.1
387 Roe GH (2005) Orographic precipitation. Annu Rev Earth Planet Sci 33(1):645–671.
388 https://doi.org/10.1146/annurev.earth.33.092203.122541

389 Shetty S, Umesh P, Shetty A (2022) Dependability of rainfall to topography and micro-
390 climate: an observation using geographically weighted regression. Theor Appl
391 Climatol 147(1–2):217–237. https://doi.org/10.1007/s00704-021-03811-w
392 Singh P, Ramasastri KS, Kumar N (1995) Topographical influence on precipitation
393 distribution in different ranges of Western Himalayas. Hydrol Res 26(4–5):259–284.
394 https://doi.org/10.2166/nh.1995.0015
395 Stuart SJ, Dean SM, Mackintosh AN, Sood A, Gibson PB, Moore S, Kendon EJ (2025)
396 Precipitation over complex mountain terrain in a convection-permitting regional
397 climate model. J Geophys Res Atmos 130(12):e2024JD042773.
398 https://doi.org/10.1029/2024JD042773
399 Suprit K, Shankar D (2008) Resolving orographic rainfall on the Indian west coast. Int J
400 Climatol 28(5):643–657. https://doi.org/10.1002/joc.1566
401 Szypuła B (2019) Quality assessment of DEM derived from topographic maps for
402 geomorphometric purposes. Open Geosci 11(1):843–865.
403 https://doi.org/10.1515/geo-2019-0066
404 Torres RN, Fraternali P, Milani F, Frajberg D (2018) A deep learning model for identifying
405 mountain summits in digital elevation model data. In: 2018 IEEE First International
406 Conference on Artificial Intelligence and Knowledge Engineering (AIKE), pp 212–

217. https://doi.org/10.1109/AIKE.2018.00049

Yin Z-Y, Zhang X, Liu X, Colella M, Chen X (2008) An assessment of the biases of satellite rainfall estimates over the Tibetan Plateau and correction methods based on topographic analysis. J Hydrometeorol 9(3):301–326. https://doi.org/10.1175/2007JHM903.1

Zaujec P, Fedor T, Halaj M, Onderka M (2025) Exploiting the windward and leeward precipitation effect of northern and northwestern cyclonic types to correct WRF numerical model predicted precipitation totals. Theor Appl Climatol 156(8):429. https://doi.org/10.1007/s00704-025-05642-5

Zhang W, An M, Chen G, Zhao F, Cheng Y, Tang J (2022) The quantification of mountain base elevation based on mountain structure modeling. Front Environ Sci 10:1030301. https://doi.org/10.3389/fenvs.2022.1030301

Figure Legends

Fig. 1 Study area and selected summit locations used in this study. The shaded colors indicate elevation based on the 25 m DEM created from GSI elevation point data. Red triangles indicate summit locations selected from the GSI list of major mountains in Japan.

Fig. 2 Conceptual diagram of the windward–leeward classification method under easterly wind conditions. Red lines indicate ridgelines within individual mountain areas, and the blue line indicates a saddle/valley boundary between adjacent mountain areas. Blue and red shaded areas indicate windward and leeward areas, respectively. Green arrows indicate wind direction.

Fig. 3 Example of the stepwise construction of summit-based mountain areas in southern Kyushu. Colored areas indicate mountain areas assigned to each summit, and black triangles indicate summit locations. As the elevation threshold decreases from (a) 1000 m to (d) 150 m, mountain areas expand from high-elevation regions around the summits toward lower-elevation areas.

Fig. 4 Example of representative-line extraction within a mountain area under easterly wind conditions. Cyan points indicate representative high-elevation points extracted from each bin, and magenta points indicate excluded points with elevations lower

than 200 m. The yellow line indicates the representative line constructed from the smoothed representative high-elevation points, and the red line indicates the classification line shifted 0.5 km leeward from the representative line. The black triangle indicates the summit location.

Fig. 5 Windward–leeward classification result under easterly wind conditions. Blue and red areas indicate windward and leeward areas, respectively, and gray areas indicate unclassified areas. Black lines indicate boundaries between adjacent mountain areas, and black triangles indicate summit locations. Numbers indicate mountain area IDs corresponding to the summit locations.

Fig. 6 Differences in mean precipitation between windward and leeward areas for each mountain area. Mountain area IDs correspond to those shown in Fig. 5. Positive values indicate greater mean precipitation on the windward side than on the leeward side. The numbers above the bars indicate the precipitation differences (windward − leeward). Blue bars indicate statistically significant differences ($p < 0.05$), whereas gray bars indicate non-significant differences, based on one-sided label-flipping permutation tests.